Available online at www.sciencedirect.com

ScienceDirect

Proceedings of the Combustion Institute 000 (2022) 1–8

Proceedings of the Combustion Institute

www.elsevier.com/locate/proci

Effects of inter-pulse coupling on nanosecond pulsed high frequency discharge ignition in a flowing mixture

Xingqian Mao [a,*], Hongtao Zhong [a], Ziyu Wang [a], Timothy Ombrello [b], Yiguang Ju [a]

[a] *Department of Mechanical and Aerospace Engineering, Princeton University, Princeton, NJ 08544, United States*
[b] *Aerospace Systems Directorate, Air Force Research Laboratory, Wright-Patterson Air Force Base, Ohio 45433, United States*

Received 5 January 2022; accepted 28 June 2022
Available online xxx

Abstract

This work numerically investigates the effects of non-equilibrium nanosecond plasma discharge pulse repetition frequency, pulse number, and flow velocity on the critical ignition volume, minimum ignition energy, and chemistry in a plasma-assisted H_2/air flow at 300 K and 1 atm using a multi-scale adaptive reduced chemistry solver for plasma assisted combustion (MARCS-PAC). The interactions between discharges/ignition kernels spanning decoupled, partially-coupled and fully-coupled regimes in a pulse train are studied. For a single pulse discharge, increased flow velocity increases the minimum ignition energy required due to the increase of convective heat loss and flame stretch. The results show that the minimum ignition kernel propagation speed at the critical ignition kernel volume increases with the flow velocity. The minimum critical ignition volume decreases with the increase of plasma discharge energy. For sequential two-pulse discharges, ignition fails at both decoupled and partially-coupled regimes even when the total discharge energy is above the minimum ignition energy, but succeeds only in the fully-coupled regime at a shorter inter-pulse time. Overlap of the OH radical pool between the sequential two-pulse discharges and the increase of the chemistry effect due to the increase of reduced electric field in the fully-coupled regime contribute to the ignition enhancement. In addition, for two-pulse discharges in the fully-coupled discharge regime, the mixture can be ignited at a total energy below the minimum ignition energy of a single pulse with the same flow conditions. Moreover, for a given total discharge energy with multiple pulsed discharges, the enhancement of the ignition kernel volume has a non-monotonic dependence on discharge frequency and pulse number. The effective ignition enhancement can be achieved with an optimal pulse repetition frequency and pulse number. This work provides a new understanding of the mechanism for repetitive plasma ignition and insights for the optimization of plasma ignition in a reactive flow.

Keywords: Plasma assisted ignition; Nanosecond pulsed high frequency discharge; Minimum ignition volume; Inter-pulse coupling; Minimum ignition energy

* Corresponding author.
E-mail address: xingqian@princeton.edu (X. Mao).

https://doi.org/10.1016/j.proci.2022.06.018

1. Introduction

Efficient ignition and flame propagation in reactive flows are critical in internal combustion engines, gas turbines and high-speed propulsion [1–5]. The competition between the heat release and radical production in the ignition kernel and the convective heat loss and radical quenching [6] due to fluid motion determines the ignition probability. Recently, the application of nanosecond pulsed high frequency discharge (NPHFD) in reactive flows [7–13] has drawn great attention. The NPHFD can generate a high reduced electric field E/N (where E is the electric field and N is the gas number density) to enhance the chemistry effect on ignition. For example, volumetric production of chemically active species, such as electronically excited species, radicals, ions and electrons as well as gas heating at high E/N by non-equilibrium excitation effects of plasma significantly enhances ignition [1,2,14,15]. Meanwhile, the nanosecond discharge at different pulse repetition frequencies (PRFs) allows for the control of energy deposition at the timescales from nanoseconds to milliseconds with various inter-pulse times (IPTs) [7]. These advantages of NPHFD significantly enhance ignition and flame propagation in reactive flows.

The experiments of Opacich et al. [8] showed that a larger kernel radius can be produced by the NPHFD compared with the conventional spark discharges with the same energy deposition in CH_4/air mixtures. Experiments conducted by Lefkowitz et al. [9,10] showed that the NPHFD PRF affected the ignition probability and minimum ignition power. In their work, three regimes as "decoupled," "partially-coupled" and "fully-coupled" of "inter-pulse coupling" were used to classify the discharge event and subsequent kernel interactions with different ignition probability. The subsequent pulses can overlap with the previous one within an IPT window. For lower PRFs, decoupled ignition kernels are formed and developed for each pulse due to convective motion. This is termed the decoupled regime. At the highest PRFs, full coupling between ignition kernels and a synergy between discharges and ignition kernels with higher E/N occur in the inter-electrode gap and produce significantly elevated temperatures greater than a single pulse discharge. The elevated temperatures can persist in the kernel and increase ignition probability as well as produce more rapid kernel growth. This is termed the fully-coupled regime. In the transition between these two distinct regimes, there are varying levels of spatial overlap between discharges/kernels. This is termed the partially-coupled regime. The results showed that the ignition probability was the highest in the fully-coupled regime with short IPT. The partially-coupled and decoupled regimes at longer IPTs had lower ignition probability. Adams et al. [16] studied the effects of inter-pulse coupling on gas temperature in NPHFD via spectroscopy of the $N_2(C\rightarrow B)$ emission. The results showed that the discharges within the burst were thermally coupled at frequencies above 10 kHz, and temperatures in excess of 7000 K were possible with pulse coupling at high PRFs. Lefkowitz et al. [7] measured the OH concentration in NPHFD by planar laser-induced fluorescence (PLIF). They found that the higher PRF accelerated OH accumulation in the inter-electrode region. The discharge pulses overlapping with the developing ignition kernel are directly correlated with high ignition probability.

The above experiments showed that the ignition enhancement was the most efficient in the fully-coupled regime due to the strongest inter-pulse chemistry coupling effects. However, how nanosecond discharges affect the ignition enhancement in different regimes of inter-pulse coupling is still not clear. It is also uncertain whether there exists an optimal ignition enhancement by the PRF and number of pulses in a reactive flow. The experiments of Lovascio et al. [17] showed that the ignition time was minimized for a certain PRF corresponding to the largest synergy between pulses in quiescent lean propane/air mixtures. Their results showed the mean rate of energy deposition was a key defining parameter to optimize ignition enhancement. Similar results of the high non-monotonic dependence of ignition probability versus PRF were also observed by Shy et al. [18] and Nguyen et al. [19] experimentally. Wang et al. [20] conducted 1D simulations to study the forced ignition process using non-equilibrium plasma generated by NPHFD in a quiescent environment. The results showed the ignition process was strongly affected by the characteristics of nanosecond pulsed discharge, including pulse number, discharge frequency and total input energy. Since flow significantly modifies the ignition kernel development, flame stretch, heat loss, and radical quenching, it is necessary to understand the inter-pulse coupling effects on ignition enhancement for flowing mixtures. However, such modeling is very challenging because it requires resolving chemistry and transport in both temporal (ns-ms) and spatial (μm-cm) scales. Recently, a new two-dimensional multi-scale adaptive reduced chemistry solver for plasma assisted combustion (MARCS-PAC) was developed and validated [21,22]. The model integrates the experimentally validated 2D plasma solver PASSKEy (PArallel Streamer Solver with KinEtics) [23–25] and the Adaptive Simulation of Unsteady Reactive Flow solver ASURF+ [26–28]. This solver provides a validated computational platform for modeling plasma-assisted reactive flows and offers great opportunities to study the inter-pulse coupling effects.

The objective of this work is to numerically study the effects of inter-pulse coupling during a

Please cite this article as: X. Mao, H. Zhong, Z. Wang et al., Effects of inter-pulse coupling on nanosecond pulsed high frequency discharge ignition in a flowing mixture, Proceedings of the Combustion Institute, https://doi.org/10.1016/j.proci.2022.06.018

repetitive nanosecond pulsed high frequency discharge ignition in reactive flows. The modeling is conducted by the 2D MARCS-PAC solver. Firstly, the effects of flow velocity on the minimum discharge energy and ignition kernel propagation with a single discharge pulse are studied. Then, the synergistic effects of discharges on ignition kernel development and propagation using two sequential pulsed discharges in the decoupled, partially-coupled and fully-coupled regimes are investigated, respectively. The interactions between the plasma discharge and ignition kernel formation are discussed. Finally, the effects of pulse repetition frequency and pulse number with a fixed total discharge energy on ignition enhancement are studied. The optimal characteristics of NPHFD are discussed.

2. Numerical methods

The numerical modeling is conducted by the two-dimensional multi-scale adaptive reduced chemistry solver for plasma assisted combustion (MARCS-PAC) recently developed at Princeton University [21,22]. The drift-diffusion-reaction equations for plasma species, Helmholtz equations for photoionization, Poisson equation for electric field, energy conservation equation for plasma discharge and unsteady, multi-component, reactive, compressible Navier-Stokes (N-S) equations are coupled by time splitting solution methods. The governing equations and numerical schemes were described in detail in [21,22].

In this work, all the simulations are conducted in a fuel rich H_2/air (0.627 H_2/0.078 O_2/0.295 N_2) mixture with an equivalence ratio of $\varphi = 4.0$ (the Lewis number *Le* is $\sim$ 2.2 [26]) at 300 K and atmospheric pressure. To observe the impact of ignition energy on the flame kernel propagation, a hydrogen fuel-rich mixture whose Lewis number is greater than one with smaller kinetic mechanism is chosen to mimic the fuel-lean conditions of large hydrocarbon fuels, which also have a mixture Lewis number greater than one. To initiate the discharge, a uniform pre-ionized $H_2/O_2/N_2$ mixture with a low initial electron number density of 10^4 cm^{-3} is used in the simulation [29]. The initial ion densities are given based on quasi-neutrality. A trapezoidal waveform voltage with a peak value of 9000 V and a rise time of 2 ns was applied to the electrodes according to the experimental conditions of Lefkowitz et al. [9]. For comparing the efficiency of NPHFD on ignition, it is assumed the deposited energy in each pulse is constant. The discharge duration of each pulse is adjusted by holding a constant deposited energy in the plasma for all simulations. The plasma assisted $H_2/O_2/N_2$ combustion kinetic model from our previous work [22] is used. The model consists of a plasma sub-model and a combustion sub-model.

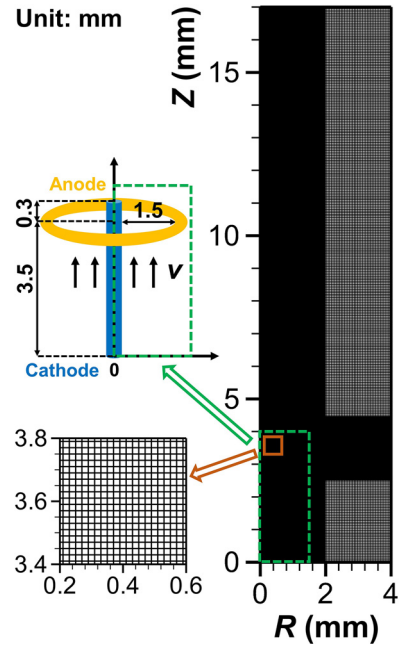

Fig. 1. 2D computational domain, geometry and mesh distribution.

The plasma sub-model incorporates the reactions involving electronically excited species $O_2(a^1\Delta_g)$, $O_2(b^1\Sigma_g^+)$, $O(^1D)$, $N_2(A)$, $N_2(B)$, $N_2(a')$, $N_2(C)$, $N(^2D)$; ions H_2^+, O_2^+, N_2^+, N_4^+, O^-, O_2^- and electrons. The vibrationally excited species are consumed by vibrational-translational (VT) relaxation reactions and provide gas heating to the mixture [2]. The rate constants of electron impact reactions, the mean electron energy and the transport parameters for electrons are pre-calculated by BOLSIG+ [30]. The cross-section data of electron impact reactions are obtained from the online database LXcat [31]. The reaction cross-sections of H_2 and N_2 are obtained from the Phelps database [32], and the cross-section data of O_2 are taken from the Biagi database [33]. The ionization cross-sections of H_2 are obtained from the IST-Lisbon database [34] which provides more detailed data at different electron energies. The electron temperature in the plasma discharge is obtained by solving the Boltzmann equations with the local field approximation [35]. A detailed $H_2/O_2/N_2$ combustion mechanism from HP-Mech [36] with NO_x formation [37,38] and O_3 sub-mechanisms [39] was used in the combustion sub-model.

Fig. 1 shows the 2D computational domain, geometry and mesh distribution. Axisymmetric needle-to-ring electrodes were used in this study. Note that plasma discharge between the ring and the needle will not be exactly uniform, but for simplification was assumed to be uniform for this

Please cite this article as: X. Mao, H. Zhong, Z. Wang et al., Effects of inter-pulse coupling on nanosecond pulsed high frequency discharge ignition in a flowing mixture, Proceedings of the Combustion Institute, https://doi.org/10.1016/j.proci.2022.06.018

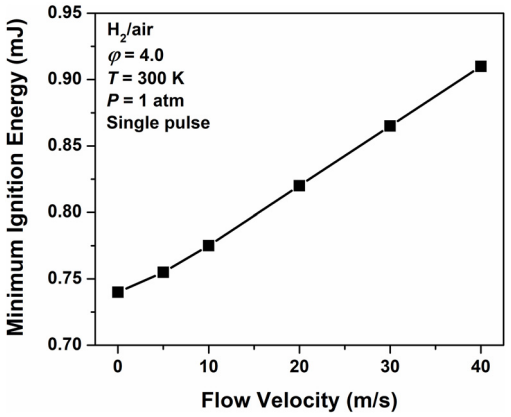

Fig. 2. Minimum ignition energy (MIE) at different velocities with a single nanosecond discharge pulse.

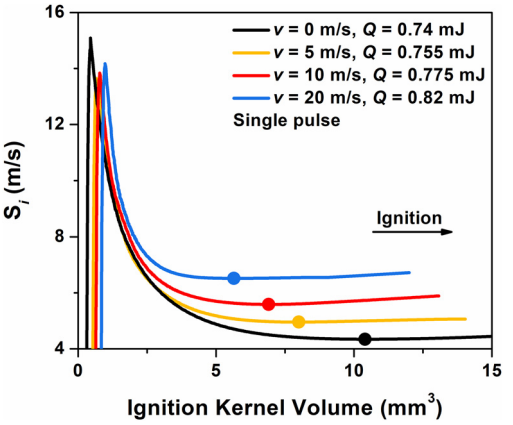

Fig. 3. Ignition kernel propagation speed S_i as a function of ignition kernel volume at different flow velocities with minimum ignition energy. The circle in each case indicates the critical ignition kernel volume.

parametric study. To reduce the complexity of 3D plasma modeling and focusing on the kinetic effect of plasma discharge on ignition, we assume that the plasma discharge is also axisymmetric. The R-axis indicates the direction of electrode radius and the Z-axis indicates the direction of needle electrode length and gas flow of the cylindrical coordinates. The length of needle electrode in the computational domain is 3.8 mm. The gap size between needle and ring electrodes is 1.5 mm. The ring electrode is placed at the position of 0.3 mm below one end of the needle electrode to prevent the extremely high electric field generated near the sharp electrode edges. The radius of the needle and ring electrodes is set as 60 μm and 40 μm, respectively, to reduce the flow recirculation near the electrodes. To reduce the computational cost, a fine and uniform orthogonal mesh (20 μm $\times$ 20 μm) is used in the plasma discharge region, and the largest mesh size is 50 μm $\times$ 50 μm in the outer region. The high voltage is applied to the ring electrode and the needle electrode is connected to the ground. The time step is determined by the shortest characteristic timescale of the drift dynamics of charged species, plasma kinetics, combustion kinetics and fluid dynamics for all grids.

3. Results and discussion

3.1. Effects of flow velocity on the minimum ignition energy and volume for a single pulse discharge

Fig. 2 shows the dependence of the minimum ignition energy (MIE) on the flow velocities ($v = 0$, 5, 10, 20, 30 and 40 m/s). At each flow velocity condition, the ignition and the flame propagation are calculated by varying the simulated discharge energy with an interval of 0.005 mJ. The MIE at different velocities in Fig. 2 is obtained at the minimum discharge energy for successful ignition and flame propagation. The results show that the MIE increases monotonically with the flow velocity [6,40].

To study the effects of flow velocity on ignition kernel propagation, the average propagation speed (S_i) of the ignition kernel as a function of the kernel volume is calculated. The ignition kernel volume is defined as the integration of the volume with temperature over 1000 K. The S_i is calculated by $S_i = \dot{m}/(A\rho_i)$, where $\dot{m}$ is the mass consumption rate of H_2, A is the cross section of the ignition kernel with temperature above 1000 K, and ρ_i is the mass density of burned gas at 1000 K. Fig. 3 shows the ignition kernel propagation speed as a function of the kernel volume at the MIE by a single pulse at different flow velocities ($v = 0$–20 m/s). The results show that S_i first increases significantly at a small ignition kernel volume generated by the nanosecond plasma discharge. Then, the ignition kernel propagation speed decreases as the flame propagates outwardly and reaches the minimum at the critical kernel volume. The flame propagation speed will increase and ignition is successfully achieved after the ignition kernel passes the critical volume [41,42]. Fig. 3 shows that for successful ignition, with the increase of flow velocity the propagation speed S_i increases at the critical ignition kernel. This is because at a higher flow velocity both the flame stretch ($Le > 1$) and convective heat loss increase. As a result, a larger discharge energy is required for successful ignition at higher flow velocities [6,40]. It is interesting to note that different from the conclusion of the MIE obtained in a quiescent mixture which is proportionally dependent on the critical ignition radius [41], in reactive flows the critical ignition volume can decrease

Please cite this article as: X. Mao, H. Zhong, Z. Wang et al., Effects of inter-pulse coupling on nanosecond pulsed high frequency discharge ignition in a flowing mixture, Proceedings of the Combustion Institute, https://doi.org/10.1016/j.proci.2022.06.018

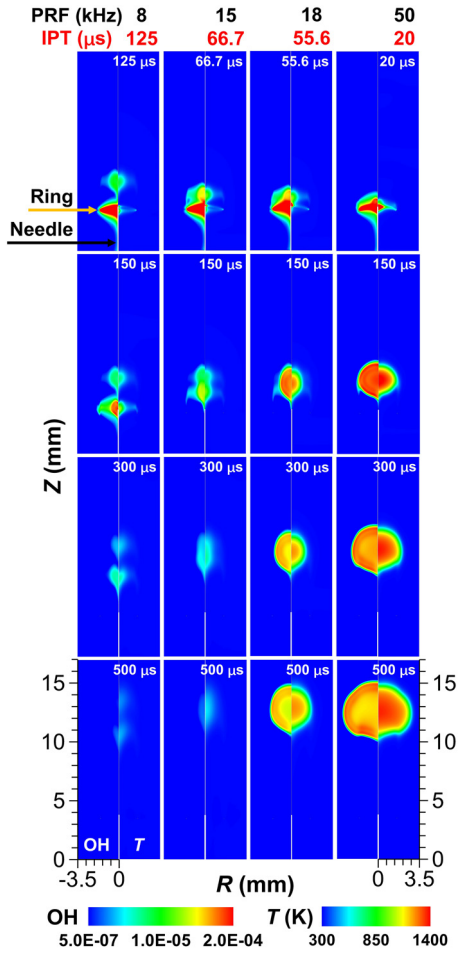

Fig. 4. Time evolutions of mole fractions of OH (left) and temperature (right) in 20 m/s flowing H_2/air mixtures at various pulse repetition frequency (PRF)/inter-pulse time (IPT) conditions with 2 pulses, respectively, at decoupled (8 kHz), partially-coupled (15 kHz) and fully-coupled (18–50 kHz) regimes. The yellow arrow indicates the location of ring electrode. The vertical white region at the bottom indicates the needle electrode.

with the increase of the MIE as the flow velocity is increased.

3.2. Effects of inter-pulse time on ignition kernel development for two sequential discharges

To study the discharge synergistic effects of inter-pulse coupling on ignition, two sequential pulses with the same discharge energy but different IPTs with a flow velocity of 20 m/s are examined. The discharge energy in each pulse is set as $Q = 0.6$ mJ, which is below the MIE of 0.82 mJ. Fig. 4 shows the time evolutions of mole fractions of OH (left) and temperature (right) at PRF = 8, 15, 18 and 50 kHz. Images in the first row show the OH distribution and temperature profiles immediately after the second pulse with the IPT of 125, 66.7, 55.6 and 20 μs, respectively. At 8 kHz, the first ignition kernel moves downstream far enough due to flow motion before the second discharge pulse. The fresh gas mixture flows to the discharge gap and another ignition kernel is generated. Two independent ignition kernels are generated at $t = 150$ μs and propagate separately. This case is in the decoupled regime of inter-pulse coupling. The results show that both ignition kernels quench at $t = 500$ μs due to cooling and dissipation. At 15 kHz, the results of OH concentration at $t = 66.7$ μs show that a part of the discharge volume generated at the second pulse overlaps with the previous ignition kernel. This condition is in the partially-coupled regime. The ignition kernels generated in the two pulses merge partially and form a larger ignition kernel at $t = 150$ μs. However, the ignition kernel is smaller than the critical ignition volume and thus quenches with flow motion even though the total discharge energy is greater than the MIE. Two reasons cause this: first, the relatively long IPT of 66.7 μs leads to heat loss and radical quenching during the inter-pulse period. Second, the pressure wave generated by the following ignition kernel increases the flow velocity due to expansion, leading to more convective heat loss before the two ignition kernels merge. Therefore, the merged ignition kernel fails to reach the critical ignition volume for flame propagation. When PRF $\geq$ 18 kHz, the second pulse is coupled fully with the first ignition kernel. These cases are in the fully-coupled regime. The successful ignition and flame propagation occur both at 18 and 50 kHz. The results show that the larger ignition kernel is formed with shorter IPT. In summary, the discharge pulse must overlap with the developing ignition kernel in the inter-electrode region to achieve effective ignition.

To further compare the interactions between plasma discharge and ignition kernel in different regimes, the mole fractions of OH in the electrode gap immediately after the second discharge are shown in Fig. 5. The results show that the OH concentration significantly increases at 50 kHz due to the overlap of the second pulse with the first ignition kernel. This leads to pumping of radicals with the second pulse and faster OH accumulation and therefore a larger ignition kernel at a high PRF. At 8 kHz, the PRF is too low to accumulate OH. As the ignition kernel generated in the discharge volume also affects the following discharge characteristics, the E/N values after the second pulse breakdown are shown in Fig. 5. At 8 kHz, Fig. 5(a) shows that the E/N distribution is uniform in the discharge gap. This is because a fresh gas mixture flows to the electrode gap in each pulse with a long IPT of 125 μs, and E/N distribution remains unchanged. However, the E/N values significantly increase at the second pulse of 50 kHz when the plasma dis-

Please cite this article as: X. Mao, H. Zhong, Z. Wang et al., Effects of inter-pulse coupling on nanosecond pulsed high frequency discharge ignition in a flowing mixture, Proceedings of the Combustion Institute, https://doi.org/10.1016/j.proci.2022.06.018

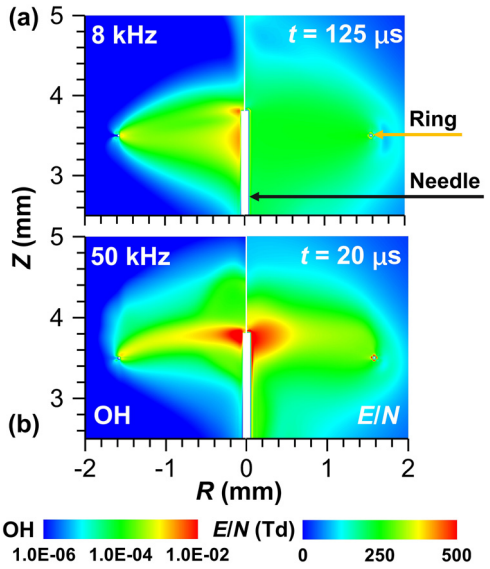

Fig. 5. Mole fractions of OH (left) and E/N values (right) in the electrode gap after the second pulse breakdown at (a) 8 and (b) 50 kHz (1 Td = 10^{-17} V cm^2). The yellow arrow indicates the location of ring electrode. The vertical white region at the bottom indicates the needle electrode.

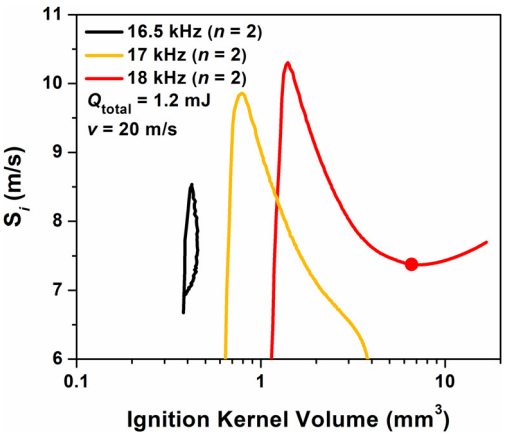

Fig. 6. Ignition kernel propagation speed S_i as a function of ignition kernel volume in 20 m/s flowing H_2/air mixtures at PRF = 16.5, 17, and 18 kHz with 2 pulses. The circle in each case indicates the critical ignition kernel volume, which was only achieved at 18 kHz.

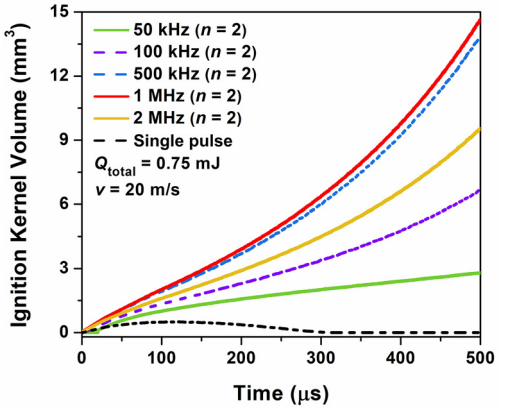

Fig. 7. Time evolutions of ignition kernel volume in 20 m/s flowing H_2/air mixtures at different PRFs.

charge overlaps with the ignition kernel, as shown in Fig. 5(b). The flame kernel generated by the previous pulse is still in the electrode gap with the IPT of 20 μs. This increases the discharge temperature ($T\uparrow$) and reduces the gas number density ($N\downarrow$) in the second pulse. Therefore, the E/N in the discharge gap is enhanced correspondingly and the discharge transitions to a constricted type [43,44]. The increase of E/N further promotes the production of electrons as well as the concentrations of excited species and radicals. The inter-pulse coupling effects at high frequencies in the fully-coupled regime show a positive feedback on the enhancement of both plasma discharge and ignition kernel development. To summarize, the residence time of ignition kernel volume in the electrode gap is critical for successful ignition when the discharge energy in each pulse is lower than the MIE.

Fig. 6 shows S_i as the function of ignition kernel volume at PRF = 16.5, 17, and 18 kHz with two sequential pulses ($n = 2$). The frequencies at 16.5 and 17 kHz are in the partially-coupled regime and 18 kHz the fully-coupled regime. The results show that S_i increases with PRF. At 18 kHz, the ignition kernel continues expanding after reaching its critical volume and a self-sustained propagating flame is successfully initiated in the flow (shown in Fig. 4). However, at the conditions of 16.5 and 17 kHz, the ignition kernel fails to reach the critical ignition kernel volume. This again demonstrates that critical ignition volume is an important parameter for ignition kernel development and flame propagation. For ignition enhancement by NPHFD, it is more effective for the fully-coupled regime than the partially-coupled regime.

From the discussion above, we conclude the NPHFD significantly enhances ignition in the fully-coupled regime at high frequencies when the discharge overlaps with the ignition kernel effectively. However, the total discharge energy used is $Q_{\text{total}} = 1.2$ mJ which is above the MIE of 0.82 mJ at $v = 20$ m/s. The mixture can still be ignited by a single pulse with 1.2 mJ at the same flow velocity. To understand whether repetitive discharge pulses can ignite a mixture with a total discharge energy below the MIE of a single pulse, the calculations of sequential two repetitive discharges are conducted by using a total discharge energy of 0.75 mJ. Fig. 7

Please cite this article as: X. Mao, H. Zhong, Z. Wang et al., Effects of inter-pulse coupling on nanosecond pulsed high frequency discharge ignition in a flowing mixture, Proceedings of the Combustion Institute, https://doi.org/10.1016/j.proci.2022.06.018

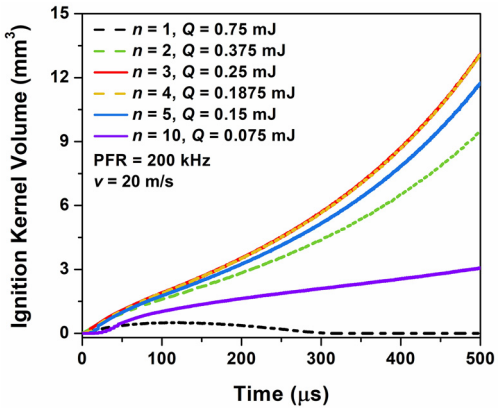

Fig. 8. Time evolutions of ignition kernel volume in 20 m/s flowing H_2/air mixtures with different pulse numbers at PRF = 200 kHz.

shows the time evolutions of ignition kernel volume in 20 m/s flowing H_2/air mixtures at different PRFs. PRFs greater than 50 kHz are in the fully-coupled regime. The pulse number is $n = 2$ and the energy of each pulse is $Q = 0.375$ mJ. The results show that the ignition kernel is quenched with a single pulse. For two pulses, the ignition kernel volume continues increasing with frequency and reaches maximum at 1 MHz. For PRF = 2 MHz, the ignition kernel volume decreases. Note that the IPT (0.5 μs) at this condition is less that the relaxation time of pressure wave from a single discharge (~ 1 μs). The gas number density (N) in the flame kernel is not reduced due to the increase of pressure and E/N values at the second pulse are not effectively promoted. When the PRF is greater than 2 MHz, the ignition efficiency decreases. It can be concluded that there exists an optimal discharge frequency for two pulses which can further reduce the minimum ignition energy than that in the single pulse case.

3.3. *Effects of pulse number on ignition kernel development at a given discharge frequency and total energy*

The effects of pulse number n are also studied by varying it between 1 and 10 at PRF = 200 kHz in the fully-coupled regime. The total discharge energy is maintained as $Q_{total} = 0.75$ mJ. The energy is split evenly into each pulse. Fig. 8 shows the time evolutions of ignition kernel volume in 20 m/s flowing H_2/air mixtures with different n. The results show that the H_2/air mixture is ignited by splitting the single pulse energy evenly to multiple pulses with the same total discharge energy. There is a non-monotonic dependence of ignition kernel volume on n. At first, the ignition kernel volume increases with n. The maximum ignition enhancement is achieved at $n = 3$. Further increase of n decreases the ignition kernel volume. From the discussion in Section 3.2, the ignition enhancement by multiple pulses is determined by the positive feedback of plasma discharge and ignition kernel development. However, the increase of pulse number also decreases the discharge energy deposited in each pulse for a fixed total energy. The ignition kernel volume significantly decreases at $n = 10$ due to the low discharge energy of 0.075 mJ in each pulse. There exists an optimal pulse number at which the energy deposition is most effective for ignition kernel development. This indicates optimal ignition by NPHFD is governed by the discharge power (PRF and energy per pulse) and total duration of a pulse train.

4. Conclusions

The effects of pulse repetition frequency (PRF), pulse number (n) and flow velocity on the critical ignition volume, minimum ignition energy (MIE) and plasma chemistry in non-equilibrium nanosecond pulsed high frequency discharge (NPHFD) ignition are numerically studied in a H_2/air mixture. The modeling is conducted by a multi-scale adaptive reduced chemistry solver for plasma assisted combustion (MARCS-PAC). For a single pulse discharge, the results show that the MIE increases with flow velocity because both the flame stretch and convective heat loss increase. The critical ignition volume in reactive flows decreases with the increase of MIE as the flow velocity is increased. The results show that the minimum ignition kernel propagation speed at the critical volume increases with flow velocity. The results by sequential two-pulse discharges show that the ignition kernel transits from the decoupled regime to partially-coupled and fully-coupled regimes by increasing PRF (reducing the inter-pulse time (IPT)). The successful ignition is achieved at the fully-coupled regime while the ignition kernel quenches both in decoupled and partially-coupled regimes even when the total deposited energy is higher than the MIE of a single pulse discharge. It is shown that the ignition enhancement in the fully-coupled regime is contributed by both the overlap of OH radical pool and the increase of chemistry effect due to the increase of reduced electric field. The mixture can be ignited in the fully-coupled regime by the sequential two-pulse discharge even when the total energy is lower than the MIE of a single pulse with the same flow velocity. For the discharge at given a PRF and n with the same total energy, it is found that there is a non-monotonic dependence of ignition kernel volume on PRF and n. There exists an optimal PRF and n to achieve the most effective ignition enhancement, indicating that optimal ignition by NPHFD is governed by discharge power (PRF and energy per pulse) and total duration of a pulse train.

Please cite this article as: X. Mao, H. Zhong, Z. Wang et al., Effects of inter-pulse coupling on nanosecond pulsed high frequency discharge ignition in a flowing mixture, Proceedings of the Combustion Institute, https://doi.org/10.1016/j.proci.2022.06.018

Declaration of Competing Interest

The authors declare that they have no known competing financial interests or personal relationships that could have appeared to influence the work reported in this paper.

Acknowledgements

This project is supported by the NSF grants CBET 1903362, DOE grant DE-SC0020233 of Plasma Science Center, and ONR STTR grant on plasma ignition.

References

[1] Y. Ju, W. Sun, *Prog. Energy Combust. Sci* 48 (2015) 21–83.
[2] A. Starikovskiy, N. Aleksandrov, *Prog. Energy Combust. Sci.* 39 (2013) 61–110.
[3] J.B. Heywood, *Internal Combustion Engine Fundamentals*, McGraw-Hill, 1988.
[4] M.P. Boyce, *Gas Turbine Engineering Handbook*, 4th ed., Elsevier, Oxford, UK, 2012.
[5] S.G. Tuttle, C.D. Carter, K.-.Y. Hsu, *J. Propul. Power* 30 (2014) 576–591.
[6] D.R. Ballal, A.H. Lefebvre, *Symp. (Int.) Combust.* 15 (1975) 1473–1481.
[7] J.K. Lefkowitz, S.D. Hammack, C.D. Carter, T.M. Ombrello, *Proc. Combust. Inst.* 38 (2021) 6671–6678.
[8] K.C. Opacich, T.M. Ombrello, J.S. Heyne, J.K. Lefkowitz, R.J. Leiweke, K. Busby, *Proc. Combust. Inst.* 38 (2021) 6615–6622.
[9] J.K. Lefkowitz, T. Ombrello, *Combust. Flame* 180 (2017) 136–147.
[10] J.K. Lefkowitz, T. Ombrello, *Combust. Flame* 193 (2018) 471–480.
[11] Y. Bechane, B. Fiorina, *Proc. Combust. Inst.* 38 (2021) 6575–6582.
[12] D.A. Lacoste, D.A. Xu, J.P. Moeck, C.O. Laux, *Proc. Combust. Inst.* 34 (2013) 3259–3266.
[13] J.A.T. Gray, D.A. Lacoste, *Combust. Flame* 199 (2019) 258–266.
[14] X. Mao, Q. Chen, A.C. Rousso, T.Y. Chen, Y. Ju, *Combust. Flame* 206 (2019) 522–535.
[15] X. Mao, A. Rousso, Q. Chen, Y. Ju, *Proc. Combust. Inst.* 37 (2019) 5545–5552.
[16] S. Adams, J. Miles, T. Ombrello, R. Brayfield, J. Lefkowitz, *J. Phys. D: Appl. Phys.* 52 (2019) 355203.
[17] S. Lovascio, T. Ombrello, J. Hayashi, et al., *Proc. Combust. Inst.* 36 (2017) 4079–4086.
[18] S.S. Shy, Y.R. Chen, B.L. Lin, A. Maznoy, *Combust. Flame* 231 (2021) 111506.
[19] M.T. Nguyen, S.S. Shy, Y.R. Chen, B.L. Lin, S.Y. Huang, C.C. Liu, *Proc. Combust. Inst.* 38 (2021) 2801–2808.
[20] Y. Wang, P. Guo, H. Chen, Z. Chen, *J. Phys. D: Appl. Phys.* 54 (2021) 065502.
[21] X. Mao, H. Zhong, Y. Ju, *AIAA Scitech 2022 Forum* (2022).
[22] X. Mao, H. Zhong, T. Zhang, A. Starikovskiy, Y. Ju, *Combust. Flame* 240 (2022) 112046.
[23] Y. Zhu, X. Chen, Y. Wu, S. Starikovskaia, *PASSKEy Code [software]*, Science and Technology of Plasma Dynamics Laboratory, Xi'an, China and Laboratoire de Physique des Plasmas, Paris, France, 2021 Available from http://www.plasma-tech.net/parser/passkey/ .
[24] Y. Zhu, X. Chen, Y. Wu, et al., *Plasma Sources Sci. Technol.* 30 (2021) 075025.
[25] Y. Zhu, S. Shcherbanev, B. Baron, S. Starikovskaia, *Plasma Sources Sci. Technol.* 26 (2017) 125004.
[26] Z. Chen, M.P. Burke, Y. Ju, *Proc. Combust. Inst.* 32 (2009) 1253–1260.
[27] W. Sun, *Developments of Efficient Numerical Methods for Combustion Modeling with Detailed Chemical Kinetics*, The Dept. of Mechanical and Aerospace Engineering, Princeton University, Princeton, NJ, 2020 Ph.D. Dissertation.
[28] T. Zhang, W. Sun, L. Wang, Y. Ju, *Combust. Flame* 200 (2019) 342–353.
[29] S. Pancheshnyi, *Plasma Sources Sci. Technol.* 14 (2005) 645–653.
[30] G.J.M. Hagelaar, L.C. Pitchford, *Plasma Sources Sci. Technol.* 14 (2005) 722–733.
[31] S. Pancheshnyi, S. Biagi, M.C. Bordage, et al., *Chem. Phys* 398 (2012) 148–153.
[32] Phelps database, www.lxcat.net, retrieved on July 1, 2020.
[33] Biagi database, www.lxcat.net, retrieved on July 1, 2020.
[34] IST-Lisbon database, www.lxcat.net, retrieved on July 1, 2020.
[35] M. Černák, T. Hoder, Z. Bonaventura, *Plasma Sources Sci. Technol.* 29 (2020) 013001.
[36] X. Yang, X. Shen, J. Santner, H. Zhao, Y. Ju, Princeton HP-Mech. http://engine.princeton.edu/mechanism/HP-Mech.html, 2017.
[37] H. Zhao, L. Wu, C. Patrick, et al., *Combust. Flame* 197 (2018) 78–87.
[38] P. Gokulakrishnan, C.C. Fuller, M.S. Klassen, *J. Eng. Gas Turbines Power* 140 (2018) 041509.
[39] H. Zhao, X. Yang, Y. Ju, *Combust. Flame* 173 (2016) 187–194.
[40] D.R. Ballal, A.H. Lefebvre, *Combust. Flame* 24 (1975) 99–108.
[41] Z. Chen, M.P. Burke, Y. Ju, *Proc. Combust. Inst.* 33 (2011) 1219–1226.
[42] Z. Chen, Y. Ju, *Combust. Theory Model.* 11 (2007) 427–453.
[43] H. Zhong, M. Shneider, M. Mokrov, Y. Ju, *J. Phys. D: Appl. Phys.* 52 (2019) 484001.
[44] H. Zhong, M. Shneider, X. Mao, Y. Ju, *Plasma Sources Sci. Technol.* 30 (2021) 035002.

Please cite this article as: X. Mao, H. Zhong, Z. Wang et al., Effects of inter-pulse coupling on nanosecond pulsed high frequency discharge ignition in a flowing mixture, Proceedings of the Combustion Institute, https://doi.org/10.1016/j.proci.2022.06.018